Age - Metallicity Relation in the MCs

E. Livanou[1], A. Dapergolas[2], M. Kontizas[1]

(1) *Section of Astrophysics Astronomy & Mechanics, Department of Physics, University of Athens, GR-157 83 Athens, Greece*
(2) *Institute of Astronomy and Astrophysics, National Observatory of Athens, P.O.Box 20048, GR-118 10, Greece*

Abstract: An observing program for the determination of age metallicity relation (AMR) from a study of small open LMC and SMC clusters using Stroemgren photometry has been initiated. Our goal is to trace AMR evidence and correlate them with the MC interactions and the spatial distribution of the clusters. We report on our search within 15 LMC and 8 SMC clusters scattered all over the area of these galaxies to cover a wide spatial distribution and metallicity. Fitting isochrones and Stroemgren photometry CMDs have been used in order to find the age and metallicity of their stellar content. The AMR for the LMC is displaying a gradient of metallicity, with higher metallicities towards the younger clusters. The AMR for LMC-SMC star clusters shows a possible jump of metallicity and a considerable increase at the age of about $6x10^8$yr. It is possible that this is connected to the latest LMC-SMC interaction. The AMR for the LMC is displaying a gradient of metallicity with distance from the center. The values of metallicity in SMC are found small, as expected for a metal poor host galaxy.

1. Introduction

The age - metallicity relation (AMR) is known to be very important for understanding the chemical evolution in a galaxy. LMC, our nearest galaxy, offers an ideal target for such studies not only for its proximity but for the fact that LMC, SMC and the Milky Way form a set of interacting galaxies. It is therefore important to trace the influence of this interaction on the star formation and the chemical evolution. In the LMC there is a sudden rise in the star formation rate (SFR) 2 to 4 Gyr ago (Elson et al., 1997 and Geisler et al., 1997) preceded by either a constant lower SFR (Geha et al., 1997) or possibly a virtual gap as manifested by the cluster age distribution (Da Costa, 1991, van den Bergh, 1991). The sudden rise in the SFR is also reflected in the corresponding sudden rise in the metallicity possibly connected to a former close encounter with the Milky Way which took place ~1.5 Gyr ago. The metallicity and SFR connected to this event has been observed both from [Fe/H] in the clusters (Olszewski et al., 1996, Geisler et al., 1997) and from a-particle elements in planetary nebulae (Dopita, 1997). Considering that a more recent encounter occurred 0.2 to 0.4 Gyr ago (Gardiner & Noguchi, 1996, Kunkel et al., 2000) it is very interesting to see if these two events have left their thrace in the

AMR. Dirsch et al. (2000) have determined the metallicity of six LMC populous clusters and their fields from Stroemgren photometry. They propose that their AMR predicts a less steep increase in the metallicity in earlier time than that found by Pagel & Tautvaisiene (1999).

The dramatic increase in the star formation due to the recent interaction has been revealed in the morphological evolution of the LMC and SMC (Maragoudaki et al., 1998, 2001). Therefore it seems worthwhile to investigate the AMR for the LMC and search for traces due to the previous mentioned interactions. The MCs possess a large population of stellar clusters of a whole range of ages. Small open LMC clusters offer homogeneous and ideal targets for this investigation. Their small central density, allows better statistics in the central regions. Thus we can derive cluster parameters with CCD Stroemgren photometry from small telescopes and reasonable integration times.

On the other hand the gradient in metallicity is also providing information on the chemical evolution of a galaxy. We searched for systematic radial trend of metallicity in the cluster system of the LMC (Kontizas, et al., 1993) from a sample of clusters up to 8 Kpc from the LMC centre.

In section 2 we describe the observational characteristics and data reduction while in section 3 we present the derived ages and metallicities for the clusters under investigation and discuss on our results. Our conclusions are given in section 4.

2. Observations - Reductions

Four observing runs in La Silla have been granted to this project. The LMC clusters were observed with the 1.54m Danish Telescope (Table1) using the DFOSC camera with a single 2k × 2k CCD and that was designed to match the RCA SIO 501 EX CCO (optimum final pixel size of 0."4). The full field covered by the instrument is 3.'7×13.'7. The 3.6m Telescope was turned to the SMC with the EFOSC camera. The ESO Faint Object Spectrograph and Camera (EFOSC), instrument of the ESO 3.6-m telescope, can be used as a very efficient CCD camera for wideband photometry of crowded stellar fields. EFOSC size is 1024 × 1024 pixels, with total field of view 5.'4×5.'4. The observations took place in various intervals between December 1997 and December 2002.

We used three of the Stroemgren filters y, b and v in order to be able to reach as faint as possible and search for the oldest small clusters in the LMC periphery. However it was not possible to use the u filter and/or β ones, to profit the main sequence stars as well, for the determination of the metallicity and increase our accuracy. The obtained frames have been reduced in the conventional way by DAOPHOT from both IRAF and MIDAS packages.

In each colour at least two frames were available to obtain the average magnitudes used for the CMDs and m_1 vs (b-y) diagrams. The adopted difference, in DAOPHOT mag, within the two frames is shown in Figure 1a for the cluster

Table 1 The KMHK clusters are named from Kontizas et al., (1990) whereas KMK clusters are named from Kontizas et al., (1988)

Name	RA h m s	DEC d m s	exp. Time y b v	Frames y b v	Date
KMK1	5 03 48	-69 09 44	15 30 30	2 2 2	Dec. 8,9 2002
KMK3	5 03 45	-69 05 33	15 30 30	2 2 2	Dec. 8,9 2002
KMK8	5 04 29	-69 09 21	15 30 30	2 2 2	Dec. 8,9 2002
KMK32	5 10 20	-68 52 45	15 25 30	2 2 2	Dec. 28 1998
HS153	5 10 30	-68 52 21	15 25 30	2 2 2	Dec. 28 1998
KMK49	5 21 10	-69 56 25	20 30 30	2 2 2	Jan. 3 1999
KMK50	5 21 23	-69 54 34	20 30 30	2 2 2	Jan. 3 1999
SL36	4 46 09	-74 53 19	15 30 30	2 2 2	Dec. 14,15 1999
SL620	5 36 29	-74 24 18	15 30 30	2 2 2	Dec. 16 1999
KMHK81	4 45 13	-75 07 00	15 30 30	2 2 2	Dec. 8,9 2002
KMHK1042	5 31 00	-74 40 18	15 30 30	2 2 2	Dec. 10 2002
KMHK1278	5 43 28	-63 24 47	15 30 30	2 2 2	Dec. 29 1998
KMHK1381	5 48 21	-63 35 50	15 30 30	2 2 2	Jan. 1 1999
KMHK1339	5 45 06	-70 14 30	15 30 30	2 2 2	Dec. 9 2002
KMHK1640	6 04 48	-75 06 09	15 30 30	2 2 2	Dec. 10 2002
L11(K7)	0 27 45	-72 46 53	10 15 32.5	3 3 3	Aug. 22-23 2001
L17 (K13)	0 35 42	-73 35 51	10 15 32.5	3 3 3	Aug. 22-23 2001
L113	1 49 29	-73 43 42	10 15 32.5	3 3 3	Aug. 22-23 2001
NGC376	1 03 50	-72 49 34	10 15 32.5	3 3 3	Aug. 22-23 2001
NGC419 (L85)	1 08 29	-72 53 12	10 15 32.5	3 3 3	Aug. 22-23 2001
NGC330	56 19 0	-72 27 50	10 15 32.5	3 3 3	Aug. 22-23 2001
L80	1 07 28	-72 46 10	10 15 32.5	3 3 3	Aug. 22-23 2001
NGC361	1 02 11	-71 36 21	10 15 32.5	3 3 3	Aug. 22-23 2001

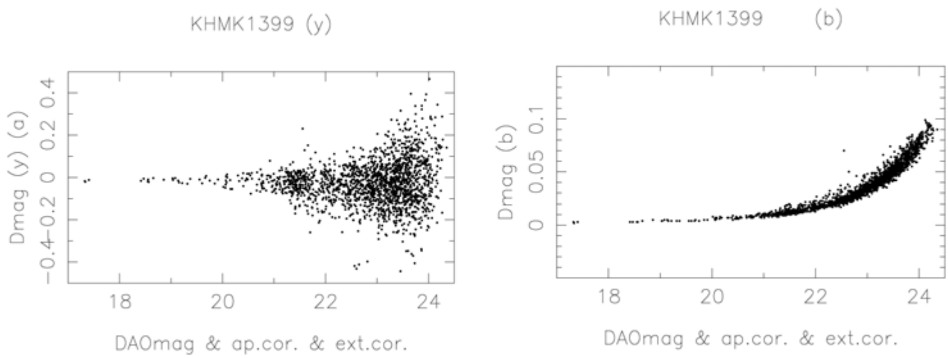

Figure 1a (Left) The adopted difference in DAOPHOT mag within the two frames for the cluster KMHK1399 for the y colour.
b (Right) The adopted DAOPHOT standard error for the cluster KMHK1399 in the y mag.

KMHK1399 in the y mag. A typical diagram of the standard error derived by DAOPHOT for the filter y of cluster KMHK1399 is shown in Figure 1b. In the case of SMC three frames are used to derive the standard error for each filter.

The adopted criteria for the CMDs are: a) During cross identification of stars on all available frames in all filters, only those stars with coordinates matching to better than 1 pixel (0.4 arcsec/pixel) were accepted. b) Photometric error for y, b, v is found as the weighted average of the values found in the corresponding frames. We used these errors to determine the final errors in (b-y) and m_1. c) The stars adopted for the production of the CMDs are only those with error 0.1mag in V, (b-y) and m_1. d) Using DAOPHOT we adopted as goodness of the PSF fit $x^2<1.9$ and image sharpness, s, |s|<1.

An appropriate set of standard stars was obtained each night in order to achieve a reliable calibration. Transformations from the instrumental system to the standard system was obtained using the equations (2.1) to (2.3), from Richter et al., (1999).

$$y_{inst} = V_{st} + A_y + B_y * X_y + C_y *(b - y)_{st} \quad (2.1)$$

$$b_{inst} = b_{st} + A_b + B_b * X_b + C_b *(b - y)_{st} \quad (2.2)$$

$$v_{inst} = v_{st} + A_v + B_v * X_v + C_v *(v - b)_{st} \quad (2.3)$$

The B_y, B_b and B_v parameters are the atmospheric extinction coefficients for the y, b, and v filters. The X_y, X_b and X_v parameters are the AirMass at the three filters and they are known from the observations. The B_y, B_b and B_v are also known, thus they are kept constant in the equations and they dont have an errors. Finally using least square fittings we estimate the rest 6 parameters: A_y, A_b, A_v, C_y, C_b, and C_v.

3. Discussion

The present sample of clusters includes seven clusters (KMK1, KMK3, KMK8, HS153, KMK32, KMK49, KMK50) located in the central region of LMC and eight clusters (KMHK81, KMHK1042, KMHK1278, KMHK1381, KMHK1399, KMHK1640, SL36 and SL620) located in the outer region of the LMC. From the outermost clusters 3 are located in the north and 5 in the south with an average distance R <= 6-7 Kpc. Generally the young LMC clusters (a few times 10^8 yr) are only located in the central region, while the older ones are found all over the LMC (Kontizas et al., 1990). The spatial distribution of the MCs selected star clusters is shown in Figure 2. They are overploted on the catalogue of the MCs star clusters of Bica et al. (2008).

3.1. Ages of the clusters

For each cluster we produced a V, vs (b-y) diagram (CMD). In order to subtract the cluster stars from the contaminated nearby and/or projected field stars, we carried out the following: A central region around the cluster center was chosen, as small as possible (~0.75arcmin radius), in order to include the largest proportion of clus-

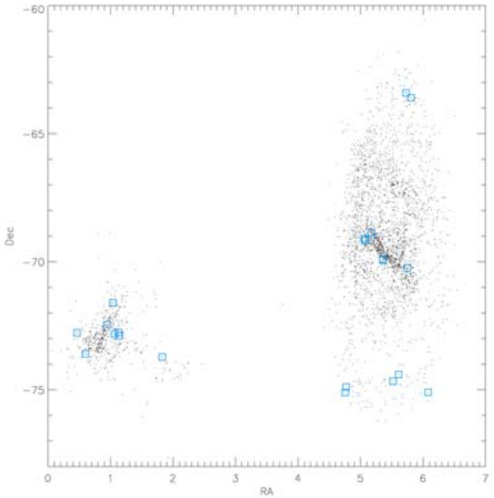

Figure 2 The spatial distribution of the MCs star clusters under investigation.

ter members and large enough, because sometime crowding was severe to have measurements of the very central stars. In the outer parts of the cluster we were able to find a region characterizing the nearby field stellar population. We selected such fields with equal area with that of the cluster and produced the corresponding CMDs. Comparison of the two diagrams (central cluster and field respectively) may allow the determination of the cluster members. In case there is a significant difference of their CMDs, the determination of the cluster parameters such as age and metallicity is much more reliable than in cases, where the two diagrams have small differences and we assume that the cluster's characteristics resemble these of the nearby field. In Figure 3 the CMD of cluster KMK1 and its adjoining field is given as an example.

The ages of the clusters have been derived from their CMDs after subtraction of the field population. The used models are those of Schaerer et al. (1993a), Schaerer et al. (1993b), Schaller et al. (1892), Charbonnel et al. (1993) with an appropriate transformation for the Stroemgren magnitudes. The comparison with the isochrones gives us the age, metallicity and the extinction for each cluster, listed in Table 2. The errors are calculated from the best fit with the models, after considering the contamination with the field stars.

3.2. Metallicities

A second set of diagrams for the cluster-field pairs was produced in order to derive the metallicity from the Stroemgren magnitudes and the traditional diagram m_1, (b-y). Hilker et al. (1995) have produced three lines of constant metallicity providing the determination of the metallicity with acceptable accuracy for the late type stars, with (b-y)>0.4. For the clusters with old ages there is a fair number of late type stars, statistically large to provide reliable metallicity. For the young clusters the

Table 2 Corresponding values Z and [Fe/H]dex (Durand et al., 1984)

Z	[Fe/H]dex
0.01	0.3
0.02	0.0
0.008	-0.5
0.004	-0.7
0.002	-1.0
0.001	-1.3

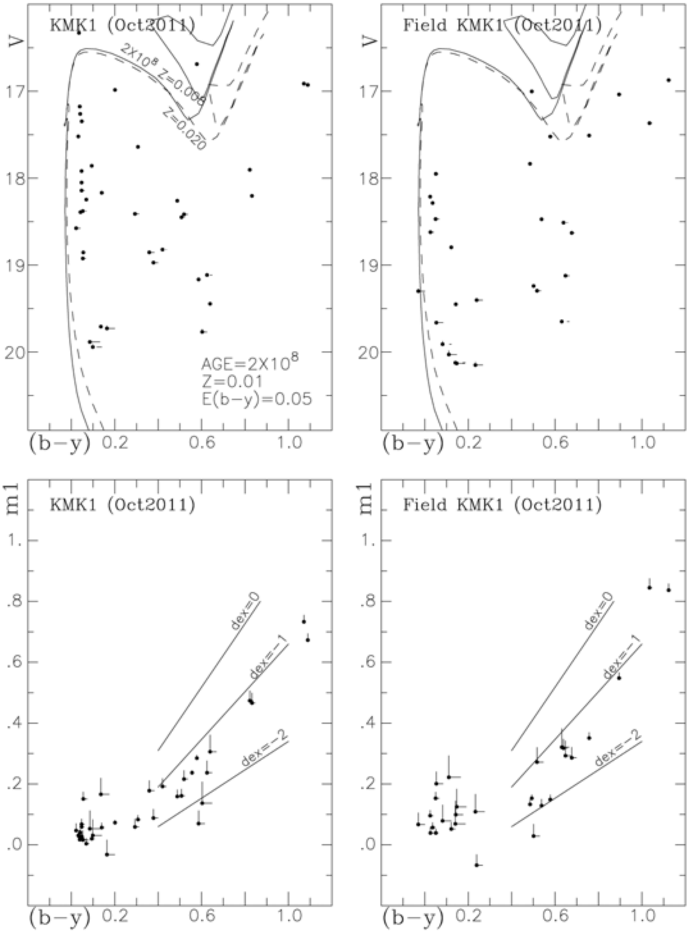

Figure 3 CMD for the cluster KMK1 and its, equal area, field for r=0.75arcmin. Metallicity for the cluster KMK1 and its field.

red giants if any are few. So the metallicity derived from m_1, (b-y) is of low accuracy and the metallicity found from the isochrones are also considered. In order to compare the two sets of metallicity values we used Table 2, where Z and the corresponding values in dex are given (Durand et al., 1984). We therefore used this table to transform Z from the isochrone fitting to dex, for clusters with poor metallicity determination from the Stroemgren colours. The pair of m_1, (b-y) diagram of KMK1 cluster and its adjoining field is shown in Figure 3 for example.

In Table 3 we give the derived characteristics for each cluster. Column 1 gives the name of the cluster, column 2, 3 lists the derived age and the corresponding error, column 4, 5, 6 and 7 give the metallicities and errors as derived from the Stroemgren magnitudes and the isochrones. Finally the last column gives the extinction as derived from the isochrone fitting.
The ages of the clusters have been derived from the CMDs at the very inner regions where contamination with field is less severe. The used models are Schaerer et al. (1993a), Schaerer et al. (1993b), Schaller et al. (1992) and Charbonnel et al. (l993).

Table 3 Derived ages and metallicities for 15 LMC and the 8 SMC star clusters

cluster	log age	[Fe/H]dex	z	E(b-y)
LMC				
KMK1	8.20	-0.25	0.010	0.05
KMK3	7.90	0.00	0.020	0.05
KMK8	8.50	-0.50	0.008	0.05
KMK32	8.30	0.00	0.020	0.00
HS153	8.30	0.00	0.020	0.00
KMK49	8.50	0.00	0.020	0.10
KMK50	8.60	0.00	0.020	0.10
SL36	9.00	-1.00	0.004	0.10
SL620	9.00	-0.50	0.004	0.05
KMHK81	9.48	-1.30	0.001	0.00
KMHK1042	9.30	-1.00	0.002	0.00
KMHK1278	8.60	-0.50	0.008	0.10
KMHK1381	8.90	-1.20	0.004	0.00
KMHK1399	9.00	-1.20	0.001	0.00
KMHK1640	9.30	-1.30	0.001	0.10
SMC				
L11	9.47	-0.80	0.001	0.05
L17	9.47	-1.20	0.001	0.00
L80	8.30	-1.00	0.004	0.00
L113	9.60	-1.70	0.001	0.00
NGC330	7.60	-1.00	0.008	0.05
NGC361	9.30	-0.80	0.004	0.00
NGC376	7.47	-1.20	0.008	0.04
NGC419	9.00	-1.00	0.008	0.03

The AMR found for the fifteen clusters is presented in Figure 4. A clear trend with higher metallicities towards the youngest clusters can be seen. The accuracy of our data is within the errors described by Hilker et al. (1995). Moreover we notice a possible jump of metallicity and a considerable increase at the age of about $6x10^8$yr. This can be connected to the latest LMC-SMC interaction which has been calculated at 10^8-10^9yr ago (Yoshizawa & Noguchi, 2003). The AMR for the LMC is also displaying evidence of a gradient of metallicity with distance from the center of the cluster, since clusters with metallicity -1.0 to -1.5 dex are mainly located at the outermost regions of the galaxy (Figure 2). On the other hand the SMC star clusters are characterised by low metallicity regardless their location on the galaxy. No clear gradient can be found in the AMR.

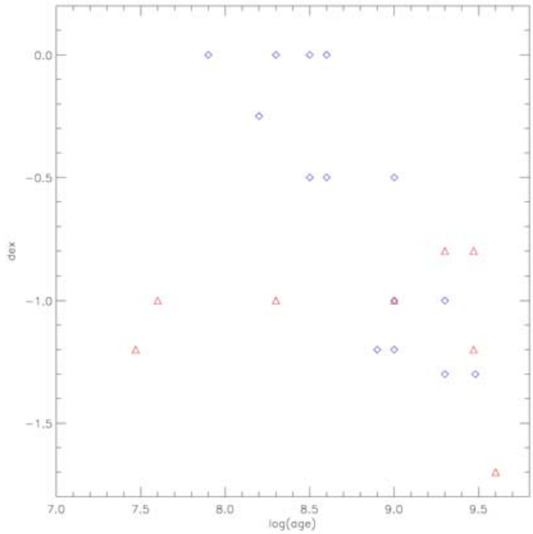

Figure 4 The age-metallicity relation for LMC (Blue Diamonds) and SMC (Red Triangles) star clusters for the age range up to 1Gyr

4. Conclusions

The age-metallicity relation (AMR) for LMC and SMC star clusters, for the age range up to 1 Gyr is investigated in this paper. The selected clusters are mainly small clusters covering distances from the center to the outer regions of both galaxies. Stromgren photometry CMDs have been used in order to find the age of their stellar content.

The AMR found for the fifteen LMC clusters shows a clear trend with higher metallicities towards the youngest clusters. A jump of metallicity and a considerable increase at the age of about $6x10^8$yr, can be assosiated with the latest LMC-SMC interaction. In the LMC clusters with metallicity -1.0 to -1.5 dex are mainly located at the outermost regions of the galaxy. In the SMC no clear trend is found in the AMR. The values of metallicity in SMC are found small, as expected for a metal poor host galaxy.

References

Bica, E., Bonatto, C., Dutra, C. M., Santos, J. F. C., 2008, MNRAS, 389, 678
Charbonnel, C., Meynet, G., Maeder, A., Schaller, G., Schaerer, D., 1993, A&AS, 101 415
Clausen, J.V., Larsen, S.S., Garcia, J.M., Gimenez, A., Strom, J., 1997, A&AS, 122 559
Da Costa, G.S., 1991 ,in IAU Symp., No 148, The Magellanic Clouds, p. 183.
Dirsch, B., Richtler, T., Gieren, W.P. Hilker, M., 2000, A&A, 360, 133
Dopita, M.A., Vassiliadis, E., Wood, P.R., et al., 1997, ApJ 474, 188
Durand, D., Hardy, E. and Melnick, J., 1984, ApJ, 283, 552.
Elson, R.W., Gilmore, G.F., Santiago, B.X., 1997, MNRAS, 289, 157.
Gardiner, L.T., Noguchi, M., 1996, MNRAS, 278, 191.
Geisler, D., Bica, E., Dottori, H., Claria, J.J., Piatti, A.E., Santos, J.F.C., 1997, AJ, 114, 1920.
Geha, M.C., Holtzman, J.A., Mould, J.R., Gallgher, J.S. III et al., 1997, astro-ph, 9711144.
Hilker, M., Richter, T., Gieven, W.P., 1995, A&A 294, 37
Kontizas, E., Metaxa, M., Kontizas, M., 1988, AJ, 96, 1625
Kontizas, M., et al., 1990, A&AS 84, 527
Kontizas, M., Kontizas, E., Michalitsianos, A.G., 1993, A&A 269, 107
Kunkel, W.E., Demers, S., Irwin, M.J., AJ, 119, 2789
Maragoudaki, F., Kontizas, M., Kontizas, E., Dapergolas, A., Morgan, D.H., 1998, A&A, 338, L29
Maragoudaki, F., Kontizas, M., Morgan, D.H., Kontizas, E., A. Dapergolas, E. Livanou, 2001, A&A, 379, 864.
Olszewski, E.W., Suntzeff, N.B., Mateo, M., 1996, Ann. Rev. Astron. Astrophys. 34, 511
Pagel BEJ and Tautvaisiene, G., 1999, Ap&SS, 265, 461
Richter, P., Hilker, M., Richtler, T., 1999, A& A, 350, 476
Schaerer, D., et al., 1993a, A&AS 102 339
Schaerer, D., Meynet, Maeder, A., Schaller, G., 1993b, A&AS, 98, 523
Schaller, G., Schaerer, D., Meynet, G., Maeder, A., 1992, A&AS, 96, 269
Schommer, R.A., 1991, in IAU Symp. No 148 The Magellanic Clouds, p 171
van den Bergh, S., 1991, ApJ, 369, 1
Yoshizawa A. & Noguchi M., 2003, MNRAS, 339, 1135